Chemical and Biological Microstructures as Probed by Dynamic Processes

J. M. DRAKE, J. KLAFTER, P. LEVITZ

The dynamic process of electronic energy transfer is shown to be an important tool for probing the microstructure of molecular systems, particularly those in which donors and acceptors occupy specifically labeled sites of spatially confining host matrices. Special attention is given to analyzing the temporal behavior of the direct energy transfer reaction for systems in which the dipolar coupling is between a donor and randomly distributed acceptors. This dynamic process is dependent on two competing lengths when the donor and acceptor distribution is determined by the microstructure of the confining system: R_p, the dominant length characterizing the size of the confinement, and R_0, which scales the strength of the dipolar coupling. When energy transfer processes are viewed in the context of these two competing lengths, a picture emerges of the microstructure of the confinement that is consistent with and corroborated by other structural probes.

THE SEMINAL WORK OF FÖRSTER ON NONRADIATIVE DIRECT electronic energy transfer (DET) between donor and acceptor molecules in condensed phases (*1*) has attracted the interest of researchers for more than four decades. Condensed matter physicists, chemists, and life scientists have investigated different aspects of the DET process for donor and acceptor molecules embedded in a broad variety of host materials ranging from liquids and solids to polymers and biochemical systems (*2–4*). The approach taken in these studies was to follow the quenching reaction of optically excited donors in the presence of ground-state acceptors, and it was sometimes possible to estimate the distances between specific sites on macromolecules when the sites were labeled with donor-acceptor pairs (*5*).

By the 1960s, DET was clearly established as a technique for studying the structure of molecular systems on scales ≤ 100 Å. Förster's proposed mechanism for DET between a donor-acceptor pair led Stryer to the concept of the "spectroscopic ruler," an idea that has proven important in establishing molecular distances in complex biological systems (*5, 6*). The use of DET as a structural tool was derived by experimental and theoretical work in biological systems. The work focused mainly on understanding steady-state experiments. Steady-state DET experiments were used in determining intermolecular distances important in various peptides (*5*), multilayers of fatty acids (*7*), and antigen-antibody complexes (*8*), and allowed researchers to determine the distributions of receptors on cell surfaces (*9*) and to establish surface density in membranes (*10*).

Recently there has been a resurgence in interest in the thermodynamic and dynamic properties of molecular systems with spatial restrictions. The types of model spatial restrictions used include zeolites, polymer membranes, porous glasses, and various molecular self-assemblies (*11–15*). One key aspect of understanding the behavior of molecular systems in confinements is establishing how the local structure of the confinement influences, or is coupled to, the thermodynamic and dynamic features of the system being studied. Therefore, making this connection between the static structure of the confinement and properties of the confined molecular system has highlighted the importance of knowing more about the geometrical features of the confinement. This is something that is frequently unclear or unknown, particularly for disordered systems such as polymers and glasses. This need to examine the microstructure has prompted investigators to apply a broad range of structural characterization techniques. The different characterization techniques are reviewed in a recent article (*16*); however, here we focus on DET and how the time-dependent rather than the steady-state characteristics of this quenching reaction can be used to study the structural features of spatial confinements. We present a new approach to understanding how the temporal features of DET are determined by the microstructure of the local environment in which the donor and acceptors are distributed. We believe that our approach to analyzing the dynamics of the DET process broadens the scope of the applicability of the concept of the spectroscopic ruler and that the temporal analysis technique, which we demonstrate using model porous glasses, can be generally applied to other systems.

DET as a Spectroscopic Ruler

The DET mechanism, as first introduced by Förster, is a dipole-dipole–dominated reaction in which an electronic excitation, initially localized on a donor (D^*), is resonantly transferred to an acceptor (A) located at distance R. This is a one-step process, with a rate $W(R)$, which we term direct energy transfer to distinguish it from the indirect process in which donor-to-donor transfer takes place before the quenching by an acceptor,

$$D^* + A \xrightarrow{W(R)} D + A^* \quad (1)$$

Förster's original theory has been extended to include general multipolar interactions as well as exchange interactions (*17*), which will not be discussed here. The donor-to-acceptor multipolar transfer rate is then

$$W(R) = \frac{1}{\tau}\left(\frac{R_0}{R}\right)^S \quad (2)$$

Here τ is the radiative lifetime of the donor in the absence of acceptors; R_0 is the critical Förster radius, which is determined by

J. M. Drake is at the Exxon Research and Engineering Company, Clinton Township, Annandale, NJ 08801. J. Klafter is in the School of Chemistry, Tel Aviv University, 69978 Tel Aviv, Israel. P. Levitz is at CNRS-CRSOCI, 45071 Orleans Cedex 2, France.

the donor-acceptor spectral overlap integral and provides an estimate of the length scale for DET; and S is the multipolar exponent: $S = 6$ for dipole-dipole, $S = 8$ for quadrupole-quadrupole interaction, and so forth. For the sake of simplicity we do not consider here anisotropic contribution to $W(R)$. The observables in DET studies are (i) the excited donor time-dependent survival probability $\Phi(t)$ in the presence of acceptors and (ii) the steady-state radiative efficiency η. These are related through

$$\eta = \frac{1}{\tau}\int_0^\infty \Phi(t)dt \tag{3}$$

A number of scenarios for DET can be addressed, each of which has an experimental realization and can be used to probe different aspects of spatial arrangements of the donor and acceptor molecules: (i) a single donor-acceptor pair, which measures a given intersite distance; (ii) a distribution of donor-acceptor pairs, which probes the intersite distribution usually related to a distribution in a macromolecule's conformations; and (iii) a donor transferring energy to a random distribution of acceptors (a minority of donors and a majority of acceptors). This scenario will be shown to be applicable to our studies of spatially confined systems.

For a single donor-acceptor pair, for which there is only one relaxation channel for the excited donor, the survival probability is given by

$$\Phi(t) = \exp[-W(R)t - t/\tau] \tag{4}$$

and therefore the radiative efficiency is

$$\eta = \frac{\tau^{-1}}{W(R) + \tau^{-1}} \tag{5}$$

In the dipole-dipole case, $S = 6$ and $\eta = R^6[R_0{}^6 + R^6]^{-1}$. Equation 5 provides the basis for deducing the distance R between a donor and an acceptor by means of efficiency measurements (R_0 can be determined independently) and has been the main idea behind applying DET as a spectroscopic ruler. Figure 1A presents schematically the labeling of sites on a macromolecule in order to obtain the end-to-end distance. Both the donor and the acceptor are assumed to be static on the time scale of the experiment. Equation 5 was successfully used in studies of a variety of biological macromolecules with different donor-acceptor pairs and different R_0 values (*5–7*) and as a standard textbook technique for studying the structure of biosystems (*18*).

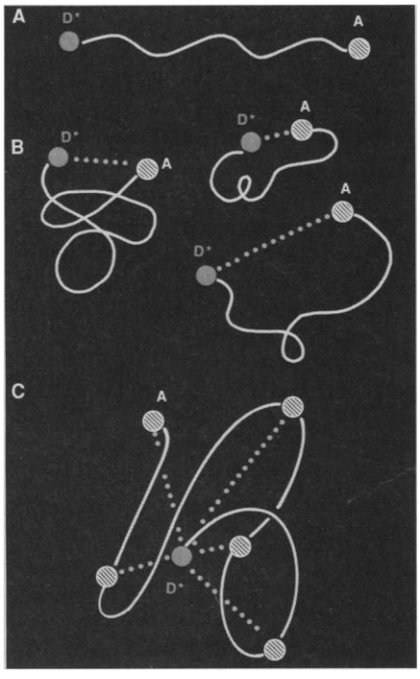

Fig. 1. Schematic presentation of different donor acceptor distributions: (**A**) a single pair; (**B**) a distribution of pairs; (**C**) a donor and randomly distributed acceptors.

Two quantities, the scaling behavior of $W(R)$ with R, $W(R) \sim R^{-S}$ in Eq. 1, and the inherent length R_0, which defines the range for DET, make DET suitable as a ruler in structural studies. The critical radius R_0 and the scaling nature of $W(R)$ play major roles in the time-dependent survival probabilities in studies of both homogeneous and restricted geometries (*11*).

In those situations where DET measurements probe more than a single donor-acceptor distance, it is necessary to introduce a distribution function $f(R)$; $f(R)dR$ expresses the fraction of donor-acceptor pairs whose separation lies between R and $R + dR$. Such distributions occur, for instance, when sites are labeled on macromolecules with a range of possible conformations (*4, 6*) as shown schematically in Fig. 1B. The survival probability is no longer a single exponential but rather

$$\Phi(t) = \exp(-t/\tau)\int f(R)\exp[-W(R)t]dR \tag{6}$$

which leads to

$$\eta = \int f(R)\frac{\tau^{-1}}{W(R) + \tau^{-1}}dR \tag{7}$$

The determination of $f(R)$, which contains the relevant structural information, from a single steady-state measurement is, of course, not possible. It was suggested (*19*) that, by using a series of different donor-acceptor pairs with different R_0 values, one could reconstruct $f(R)$ from the radiative efficiency. This procedure is tedious and somewhat limited by the narrow range of available R_0 values (usually between 15 and 60 Å).

Another possibility for deducing $f(R)$ is from time-dependent studies on a donor-acceptor pair with a fixed R_0. Here one takes advantage of the fact that the temporal measurements of $\Phi(t)$ display a broad dynamical range, contrary to a single value provided by η. Models for $f(R)$ can be then tested according to Eq. 6. Steinberg *et al.* have given a summary of the different approaches (*6*).

A different relaxation scheme, which is frequently encountered, is that of a donor being quenched by many randomly distributed acceptors. Each donor can simultaneously relax through many competing channels, as shown in Fig. 1C, a process that leads to a nonexponential decay pattern $\Phi(t)$. Unlike the previous schemes in which donor-acceptor pairs are considered, in this case for each donor there corresponds a hierarchy of donor-to-acceptor distances (*20*). Therefore, when calculating $\Phi(t)$, averaging over all possible acceptor locations is needed with the corresponding probabilities. This averaging makes the DET sense essentially the whole structure over which the acceptors are distributed. The structural details should therefore be reflected in the temporal behavior of $\Phi(t)$. The basic theoretical derivations of DET to randomly distributed acceptors are reviewed elsewhere (*11, 17*).

It was shown by Förster (*1*) that in a three-dimensional system, for dipole-dipole interaction between the donor and the randomly distributed acceptors, the survival probability is

$$\Phi(t) = \exp\left[-p\rho_0\frac{4\pi R_0{}^3}{3}\Gamma(1/2)t^{1/2}\right] \tag{8}$$

which has the functional form of a "stretched exponential," where ρ_0 is the density of acceptor sites and p is the fraction of those sites occupied and assumed to be $p << 1$; $\Gamma(X)$ is the complete gamma function. The prefactor $p\rho_0(4\pi R_0{}^3/3)$ is the number of acceptors in a sphere of radius R_0. Equation 8 has been generalized to all

Euclidean dimensions and to other multipolar interactions (*17*),

$$\Phi(t) = \exp[-p\rho_0 V_d R_0^d \Gamma(1 - d/S) t^{d/S}] \quad (9)$$

where $d = 1,2,3$, and V_d is the unit sphere in different dimensions: $V_3 = 4\pi/3$, $V_2 = \pi$, and $V_1 = 2$. The dimensionality enters into the decay form $\Phi(t)$ both through the exponent d/S and through the prefactor $p\rho_0 V_d R_0^d$. The latter gives the number of acceptors in a d-dimensional sphere of radius R_0 and therefore scales differently with R_0 for different dimensions. The strong dependencies in Eq. 9 on dimensionality make this DET scheme useful for structural studies.

The three-dimensional Förster decay form, Eq. 8, was experimentally confirmed in a large number of systems for dipolar interactions (*3, 21*). Decays in two dimension, corresponding to $d = 2$ and $S = 6$ in Eq. 9, were observed experimentally on surfaces and in molecular films (*22*). The change in the exponent of $\Phi(t)$ from 1/2 to 1/3 as the dimensionality is reduced is easily detectable. Fitting the donor's survival probability to Eq. 9 allows the dimensionality in which the DET takes place to be probed, if the multipolar exponent S is known.

The decay curves characteristic of DET from an excited donor to randomly distributed acceptors, when multipolar interactions are considered, are stretched exponentials (omitting the natural decay),

$$\Phi(t) = \exp[-At^\alpha] \quad (10)$$

where the exponent α and the prefactor A directly depend on dimensionality. When the DET is extended to restricted geometries, the decay curves maintain their stretched-exponential form and the values of α and A are determined by the structural features of the confinements. The stretched-exponential nature of $\Phi(t)$ originates from the hierarchy of donor-acceptor distances and from the scaling behavior of $W(R)$ (*20*). As will be discussed in the next section, Eq. 10 is very useful in analyzing the spatial distributions of the acceptors in DET measurements. Stretched exponentials have been shown to be a general form of relaxation patterns in a variety of fields (*23*), especially in dielectric relaxation studies in glassy systems, where these decay forms are known as the Williams-Watts decays (*20, 23*). Much effort has been expended to understand the origin of stretched exponentials and their mathematical properties (*20, 23, 24*).

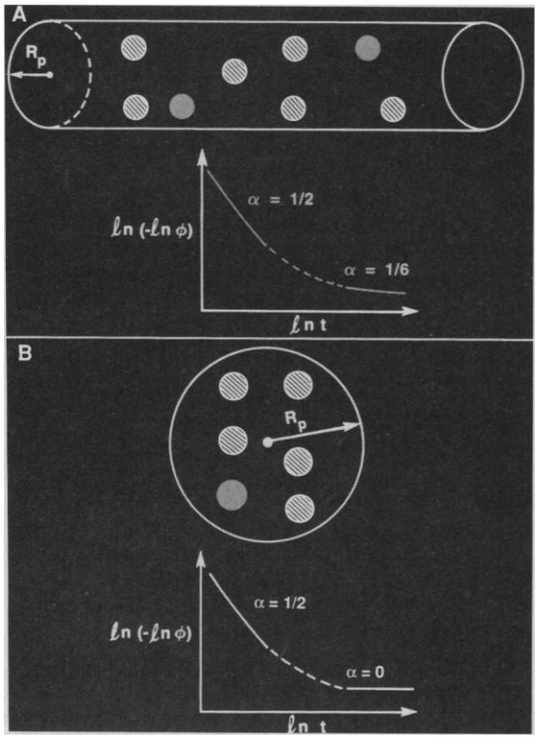

Fig. 2. Examples of spatial confinements: (**A**) a cylinder; (**B**) a sphere with the corresponding exponents of the short and long time decays according to Eq. 10.

Restricted Geometries

In homogeneous systems the role of R_0 is obvious. However, in the case of DET from a donor to randomly distributed acceptors in restricted geometries a second length enters, which characterizes the spatial restrictions. The model-restricted geometries we discuss are fractal structures, cylinders, and spheres. Although fractals introduce the concept of self-similarity, cylinders and spheres mimic the geometrical properties of pores and molecular assemblies.

In order to apply DET to these model systems, we must modify Eqs. 8 and 9 by defining a site density function $\rho(\mathbf{R})$, which describes the spatial arrangement of the acceptors around the donor. $\rho(\mathbf{R})$ is essentially the two-point correlation function on a structure.

The survival probability in the presence of acceptors is now (*11, 25, 26*)

$$\Phi(t) = \exp\{-t/\tau - p \int d\mathbf{R}\rho(\mathbf{R})[1 - \exp W(R)t]\} \quad (11)$$

A detailed discussion of Eq. 11 is given by Klafter and Blumen (*25, 26*) and by Bauman and Fayer (*27*). In the limit of an infinite system with a random acceptor distribution, $\rho(\mathbf{R}) = \rho_0$ and one recovers decays described by Eqs. 8 and 9.

Fractal structures are examples of restricted geometries. They are usually disordered, tenuous but self-similar (such as percolation clusters) (*23, 25, 28, 29*). The self-similar nature of these structures means that there is no typical length that characterizes them and so, when DET is considered, R_0 remains the dominating length. The site density function for fractals is (*30*)

$$\rho(\mathbf{R}) = \frac{F}{V_d}\rho_0\left(\frac{\bar{d}}{d}\right)R^{\bar{d}-d} \quad (12)$$

where $\bar{d}$ is the fractal dimension ($1 \leq \bar{d} \leq 3$), d is the Euclidean embedding space, and F is an unknown shape factor. The survival of a donor on a fractal is therefore (*25, 30*)

$$\Phi(t) = \exp[-t/\tau - p\rho_0 F R_0^{\bar{d}} \Gamma(1 - \bar{d}/S) t^{\bar{d}/S}] \quad (13)$$

again a stretched-exponential but with an exponent $\bar{d}/S$ that allows exponents between $d = 1$ and $d = 3$ in Eq. 9. The prefactor $p\rho_0 F R_0^{\bar{d}}$ is equal to the number of acceptors with a radius R_0 in $\bar{d}$ dimensions. Equation 13 is a generalization of the decays in regular dimensions and has been widely applied to analyze DET results in situations where Eq. 9 did not seem to apply (*11*). It has been used to interpret DET experiments on porous Vycor glass (*14*), on silica gels (*30, 31*), on zeolites (*32*), and on Langmuir-Blodgett films (*13*). It should be noted, however, that fitting decay curves to the stretched exponential in Eq. 13 may not confirm or even imply that the underlying structure is really a fractal. Behavior similar to that described by Eq. 13 with nonintegral values of $\bar{d}$ can also occur as a result of crossover processes between dimension (*33*). Nevertheless, Eq. 13 is useful in interpreting DET in restricted geometries especially when corroborated by other characterization techniques.

More conventional shapes that serve as useful models for restricted geometries are cylinders and spheres. These geometric systems are characterized by their radius R_p. When DET experiments are

performed on these geometries, it is the relation between R_0 and R_p that determines the decay patterns of $\Phi(t)$. Cylindrical pores have been used to model local pore characteristics. Many properties of porous materials are being studied in the framework of a cylindrical pore, for example, adsorption, wetting, and diffusion. Spheres are usually chosen to approximate micelle or microemulsion shapes. In order to be able to utilize DET as a tool for structural studies of these geometries, it is essential that one understand the dependence of the energy transfer reaction on the donor-acceptor distributions on or within these geometries. Figure 2, A and B, shows schematically donor and acceptor distributions on cylindrical and spherical shapes.

We first address the case of a cylinder of radius R_p with a donor and randomly distributed acceptors on its surface. Calculating the corresponding site density function and using Eq. 11, one finds (*30, 33*) that the survival probability can be numerically evaluated. Analytical expressions are easily derived for the short and long time behavior of $\Phi(t)$. The crossover time is estimated from the ratio of the two relevant length scales R_0 and R_p:

$$\Phi(t) = \exp\left[-t/\tau - p\rho_0\pi {R_0}^2\,\Gamma\left(1-\frac{2}{S}\right)(t/\tau)^{2/S}\right] \qquad (14)$$

for $t < \tau(2R_p/R_0)^S$. The short time decay displays a two-dimensional behavior according to both the exponent $2/S$ and the prefactor $p\rho_0\pi {R_0}^2$ (see Eq. 9). The donor senses only acceptors on the surface in its immediate vicinity. For long times $t > \tau(2R_p/R_0)^S$,

$$\Phi(t) = \exp[-t/\tau - p\rho_0 4\pi R_p R_0\,\Gamma(1-1/S)(t/\tau)^{1/S}] \qquad (15)$$

This corresponds to a one-dimensional relaxation according to the exponent $1/S$. The prefactor $4\pi p\rho_0 R_p R_0$ equals, for $R_p < R_0$, the number of acceptors on the cylinder surface within radius R_0. The donor's decay crosses over from a two-dimensional to a one-dimensional form at a crossover time $t_{cross} \sim (2R_p/R_0)^S$. This is a direct result of the finiteness of the systems and a fingerprint of a length, R_p, that competes with R_0. Both the short-time and the long-time decays are stretched exponentials for which the exponent and prefactor reflect the dimension and molecular arrangement of the system.

If the acceptors are now distributed within the cylinder with the donor still on the surface (*34*), then for short times $t < \tau(R_p/R_0)^S$,

$$\Phi(t) = \exp\left[-t/\tau - p\rho_0\frac{2\pi}{3}{R_0}^3\,\Gamma(1-3/S)(t/\tau)^{3/S}\right] \qquad (16)$$

a three-dimensional decay to acceptor in the volume close to the donor, but, as the prefactor indicates, the number of acceptors participating corresponds only to half a sphere of radius R_0. For long times, $t > \tau(R_p/R_0)^S$,

$$\Phi(t) = \exp[-t/\tau - p\rho_0 2\pi {R_p}^2 R_0\,\Gamma(1-1/S)(t/\tau)^{1/S}] \qquad (17)$$

characteristic of one dimension. The prefactor in Eq. 17, $2\pi p\rho_0 {R_p}^2 R_0$, is the number of acceptors in a cylinder volume of radius R_p and length determined by the critical radius R_0. Here, too, a crossover between stretched-exponential forms of the decay is predicted, but between three-dimensional and one-dimensional.

What emerges from this analysis is that DET is capable of sensing local dimensionalities as well as crossovers between them. This contributes to a more complete picture of the investigated structures. Both the exponents and the scaling of the prefactors with R_0 and R_p contain desirable information that may lead to an understanding of the morphologies of confinements. When local structures are known, the dependence of the prefactor on R_0 can provide insight about the distribution of the acceptors (see Eqs. 14 to 17 for comparison between surface and bulk locations). Crossover times, if measurable, can give clues about the typical size of the restriction, R_p.

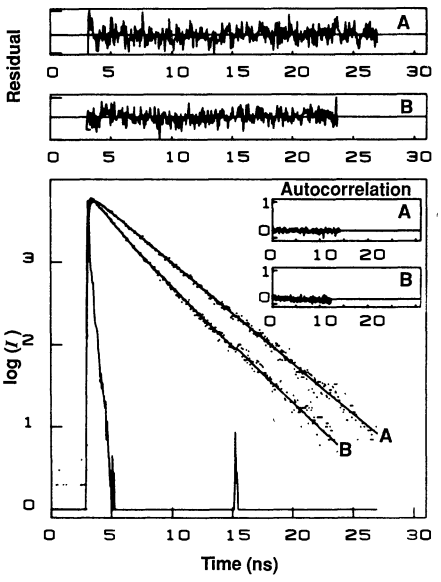

Fig. 3. Experimentally measured survival probabilities of (**A**) isolated rhodamine 6G (donor) confined to the interface of Si-500 showing an exponential relaxation corresponding to its radiative lifetime; (**B**) same system in the presence of malachite green (acceptors) showing a stretched exponential relaxation described by Eq. 19. [Adapted from (*30*) with permission of the American Institute of Physics, copyright 1988]

One arrives at the same conclusions when DET is performed on a sphere of radius R_p. If we assume that the donor and acceptors are distributed on the surface of the sphere (*30*), then for short times, $t < \tau(2R_p/R_0)^S$, we recover the same results as for the cylinder, Eq. 14. For long times we obtain

$$\Phi(t) = \exp(-t/\tau - p\rho_0 4\pi {R_p}^2) \qquad (18)$$

a simple exponential decay. The temporal behavior of $\Phi(t)$ exhibits a crossover that reflects the finiteness of the system. The same approach, based on establishing the site density function $\rho(\mathbf{R})$, can of course be used for other shapes.

The proposed procedure for analyzing experimental decays is to fit relaxation data to Eq. 10, with the two fitting parameters α and A. The exponent α is given the meaning of $\bar{d}/S$, with $\bar{d}$ as an "effective dimension," and A is proportional to the number of acceptors within a radius R_0 on the structure (and therefore should depend also on R_p). A model can then be proposed for the underlying geometry that is consistent with values of both parameters. If the apparent dimension $\bar{d}$ obtained is not an integer, then the concept of a crossover can be used in the analysis. A modified form of Eq. 10 can be applied to fit experimental decays (*30, 31*):

$$\Phi(t) = \exp[-t/\tau - A_0\,\Gamma(1-d/S)(t/\tau)^{\bar{d}/S}] \qquad (19)$$

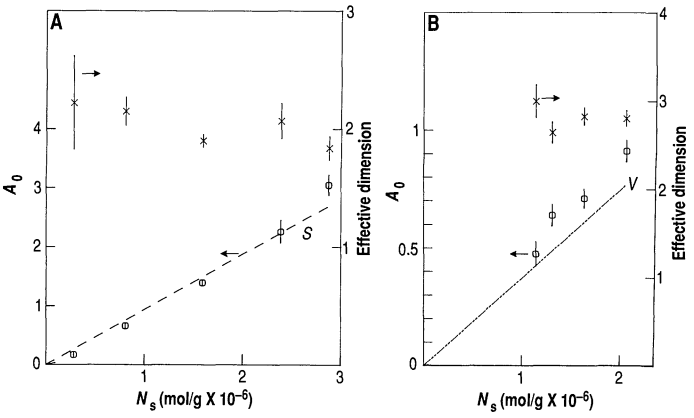

Fig. 4. (**A**) Experimental evolution of A_0 and $\bar{d}$, with the acceptor surface concentration N_s, for Si-500; the line S is the theoretical calculation of A_0 based on Eq. 21. (**B**) The same for Si-40; the line V is the theoretical calculation of A_0. [Adapted from (*30*) with permission of the American Institute of Physics, copyright 1988]

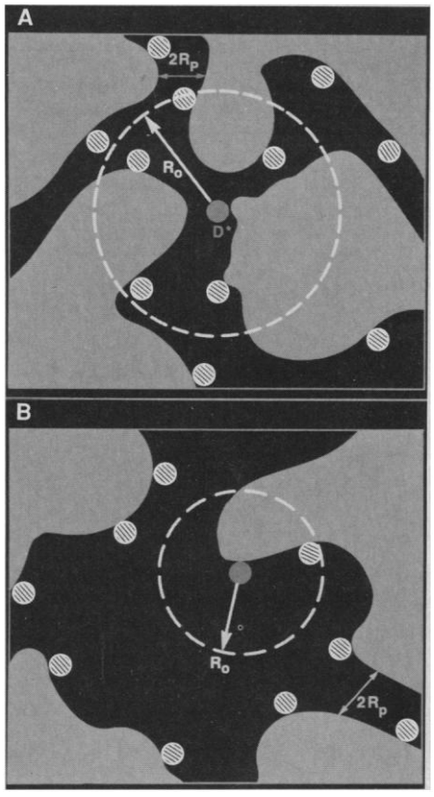

Fig. 5. Schematic representation of the two length scales R_p and R_0 for (**A**) Si-40 and (**B**) Si-500.

A straightforward connection between the static microstructure of the confinement and DET dynamics is achieved when a site density function $\rho(\mathbf{R})$ can be independently derived. Then, based on Eq. 11, dynamics and statics are directly related. Such an approach is important in establishing the method of using DET to get structural information. In a detailed study on porous Vycor glass, DET measurements and ultrathin transmission-electron-microscopy analysis of $\rho(\mathbf{R})$ were simultaneously carried out (*35*). The combined studies confirm the power of DET.

DET, using the scheme of a donor transferring energy to randomly distributed acceptors, provides insight into the microstructure of complex restricted geometries. The approach relies on stretched-exponential decays and crossover between them and the interplay between two competing lengths: R_p, inherent to the spatial restriction, and R_0, introduced by the DET method. When DET is applied to study local morphologies, corroboration with other characterization techniques is very useful, as will be described in the next section.

DET in Porous Solids and Polymer Networks

Time-dependent DET studies have been applied in a broad number of systems for the purpose of unveiling their local morphologies. These systems include porous glasses, vesicles, zeolites, polymers, and Langmuir-Blodgett films (*11–16, 27, 36, 37*). Here we review the applications to porous glasses and to networks of interpenetrating polymers, model systems with features general enough to benefit investigators in other fields.

The porous glasses investigated were a series of silica gels known as Si-40, Si-60, Si-100, and Si-500. A detailed description of these silicas is given in (*16, 30, 38*). Generally they can all be viewed as a uniform aggregation of basic building blocks with radii of the same order as their mean pore sizes R_p. Their surface areas are therefore estimated as

$$S = 3/\epsilon R_p \tag{20}$$

where ϵ is the density of silica ($\epsilon = 2.189$ g/cm^3). Knowledge of the surface areas is essential in order to define the molecular concentrations of the donors and acceptors that enter into DET considerations. The R_p values are 18 Å (Si-40), 35 Å (Si-60), 60 Å (Si-100), and 200 Å (Si-500).

The successful application of DET to probe the morphology of porous silicas has three experimental prerequisites: (i) The fluorescence decay of the adsorbed isolated donor must be monoexponential and its lifetime well defined. (ii) The critical radius R_0 of the adsorbed donor-acceptor pair must be measured independently. This permits an estimation to be made of the maximum distances probed by DET. R_0 is a critical input for understanding what one can really learn from DET. (iii) The adsorption isotherms of the donor and the acceptors must be measured. From these isotherms one can establish the range of acceptor concentrations that can be used without encountering the problems of aggregation.

Small-angle x-ray and neutron scattering results of the silica gels show that their interfaces are smooth on scales ≥10 Å (*16, 38*). These scattering results, however, do not always provide a complete picture of the local structure. In the DET experiments we used rhodamine 6G (R6G) as a donor and malachite green (MG) as the acceptors. Their R_0 on silicas was determined to be $R_0 = 57$ Å. In this system the distance sensed by DET is somewhat larger than R_0 and is determined by the experimental conditions and the acceptor concentration; we call this distance R_{max} (*30*). The higher the concentration, the smaller is R_{max} and the more local is the probed scale. We have estimated $R_{max} \sim 1.5\ R_0$ to be around 83 Å in the concentration range studied. This R_{max} then corresponds to t_{max} (~20 ns in these experiments). The dynamical behavior of the donor's decay should depend on the relation between R_{max} and the typical lengths characterizing the silicas structure, R_p. Figure 3 presents the survival probabilities, $\Phi(t)$, of the donor (R6G) on Si-500. An exponential decay is observed in the absence of acceptors ($\tau = 3.54$ ns), which turns into a nonexponential decay when acceptors are present. Such decays have been followed for a whole range of acceptor concentrations. The proposed models in the previous sections clearly predict a linear dependence on the acceptor concentrations of the prefactor, while R_0 and R_p should change for different geometries (each silica gel). Equation 19 has been used to analyze the temporal patterns of the silicas. We focus here on the large R_p (Si-500) and the small R_p (Si-40) limits. For Si-500, Eq. 19 yield $\bar{d} \sim 2$, which describes a two-dimensional DET. The relative sizes of R_{max} (or R_0) and R_p in Si-500 are such as $R_p >> R_{max}$, which, according to the model studies, should give rise to the short-time behavior, Eq. 14. The crossover time t_{cross} greatly exceeds t_{max}, which means that in Si-500 for any pore model only the local surface is "seen." The prefactor in Eq. 19 should be accordingly

$$A_0 = p\rho_0 g_{2D} \pi R_0^2 \tag{21}$$

which is the two-dimensional prefactor; g_{2D} is introduced into the data analysis to account for the anisotropy in $W(R)$ (which we ignored for simplicity) ($g_{2D} = 1.08$); $p\rho_0 = N_s/S$, where N_s is the number of acceptors per gram of the silica. From Eq. 19 $p\rho_0 = N_s\epsilon R_p/3$ and so

$$A_0 = g_{2D}\pi N_s R_p R_0^2 \epsilon/3 \tag{22}$$

Figure 4A shows the dependence of $\bar{d}$ and of A_0 on the N_s values. The $\bar{d} \sim 2$ values are confirmed and the agreement with Eq. 22 is very good.

In the case of Si-40, fits to Eq. 19 lead to $\bar{d} \sim 3$, which corresponds to a three-dimensional decay. Here $R_{max} > R_p$ and so

a crossover can be observed. Figure 4B shows $\bar{d}$ and A_0 as a function of N_s for Si-40. As modeled by a pore surface that is space-filling [see equation 41 in (*30*)], the donor is able to sense acceptors on nearby pores, probing essentially interpore DET. This explains the three-dimensional nature of $\bar{d}$ and the behavior of A_0 as a volume prefactor. The pore network in Si-40 has to branch on scales less than R_{max}. Figure 5 demonstrates schematically the different observations in Si-500 and Si-40 as the ratio R_p/R_{max} changes.

Peckan, Winnik, and Croucher used the concept of temporal crossovers to understand the underlying morphological features of interpenetrating polymer networks (*36, 37*). They used DET to examine restricted geometries within a polymer latex particle composed of two incompatible polymer materials (*36, 37*). The major component is in the form of an amorphous glass, and the minor component is a rubbery polymer. Chemical analysis indicates that all the rubbery polymer in the particle has become grafted to the major component. The rubbery phase has been labeled with fluorescent probes; by the fitting of results to Eq. 19 $\bar{d} = 2$ is obtained and modeled in terms of cylinders and thin spherical shells (*36*).

When these latex materials dissolve in solvents and are poured on a substrate, they form films that phase-separate. DET studies have been used to report on the morphologies of the composing phases. The nature of the minor component is consistent with thin cylinders, and therefore the values $1.4 \leq \bar{d} \leq 3$ correlate with different cylinder radii on the basis of crossover arguments (*37*).

Conclusions

The dynamic process of DET is an important tool for probing the microstructure of spatially confined molecular systems. We have expanded the concept of a spectroscopic ruler by placing new emphasis on the information that can be obtained from a detailed analysis of the temporal properties of the DET relaxation process. We demonstrate that, when the temporal behavior of the survival probability of the excited donor is analyzed in the context of a relaxation with a stretched exponential form, two parameters can be used to fit the data, which allow the underlying acceptor distribution to be probed. Examples are given of confined molecular systems in which DET analysis of the donor survival probability leads to both spatial and temporal crossovers. Crossovers are a key feature of DET processes in confinements. The DET process, when analyzed in the time domain, is a powerful probe of the microstructure of many types of restricted geometries.

REFERENCES AND NOTES

1. T. Förster, *Ann. Phys. (Leipzig)* **2**, 55 (1948); *Naturforscher Teil* **4**, 321 (1949).
2. L. Stryer, *Annu. Rev. Biochem.* **47**, 819 (1987).
3. D. Rehm and K. G. Eisenthal, *Chem. Phys. Lett.* **9**, 387 (1971); W. M. Yen and P. M. Selzer, Eds., *Laser Spectroscopy in Solids* (Springer, Berlin, 1981).
4. I. Ohmine, R. Silbey, J. M. Deutch, *Macromolecules* **10**, 862 (1977).
5. L. Stryer and R. P. Haugland, *Proc. Natl. Acad. Sci. U.S.A.* **58**, 719 (1967).
6. I. Z. Steinberg, E. Haas, E. Katchalski-Katzir, in *Time-Resolved Fluorescence Spectroscopy in Biochemistry and Biology,* R. B. Dundall and R. E. Dale, Eds. (Plenum, New York, 1983), pp. 411–450.
7. H. Bücher *et al.*, *Mol. Cryst.* **2**, 199 (1967).
8. E. F. Ullman *et al.*, *J. Biol. Chem.* **251**, 4172 (1976).
9. S. M. Fernandez and R. D. Berlin, *Nature* **264**, 411 (1976).
10. B. K. K. Fung and L. Stryer, *Biochemistry* **17**, 5241 (1978).
11. J. Klafter and J. M. Drake, Eds., *Molecular Dynamics in Restricted Geometries* (Wiley, New York, 1989).
12. N. Tamai *et al.*, *J. Phys. Chem.* **91**, 3503 (1987).
13. N. Tamai, T. Yamazaki, I. Yamazaki, *Chem. Phys. Lett.* **147**, 25 (1988).
14. U. Even, K. Rademann, J. Jortner, N. Manor, R. Reisfeld, *Phys. Rev. Lett.* **52**, 2164 (1984).
15. C. L. Yang, P. Evesque, M. A. El-Sayed, *J. Chem. Phys.* **89**, 3442 (1985).
16. J. M. Drake and J. Klafter, *Phys. Today* **43**, 46 (May 1990).
17. A. Blumen, *Nuovo Cimento B* **63**, 50 (1981); M. Inokuti and F. Hirayama, *J. Chem. Phys.* **43**, 1978 (1965).
18. C. R. Cantor and P. R. Schimmel, *Biophysical Chemistry, Part II* (Freeman, San Francisco, 1980).
19. C. R. Cantor and P. Pechukas, *Proc. Natl. Acad. Sci. U.S.A.* **68**, 2099 (1971).
20. J. Klafter and M. F. Shlesinger, *ibid.* **83**, 848 (1986).
21. M. G. Bennet, *J. Chem. Phys.* **41**, 3037 (1964); N. Mataga, H. Obashi, T. Okada, *J. Phys. Chem.* **73**, 370 (1969).
22. K. Kasatani, M. Kawasaki, H. Sato, *J. Phys. Chem.* **89**, 542 (1985).
23. A. Blumen, J. Klafter, G. Zumofen, in *Optical Spectroscopy of Glasses,* I. Zschokke, Ed. (Reidel, Dordrecht, The Netherlands, 1986), pp. 199–265.
24. H. F. Kauffmann, G. Landl, H. W. Engl, in *Dynamical Processes in Condensed Molecular Systems*, A. Blumen, J. Klafter, D. Haarer, Eds. (World Scientific, Singapore, 1990), pp. 90–94.
25. J. Klafter and A. Blumen, *J. Chem. Phys.* **80**, 874 (1984).
26. ———, *J. Lumin.* **34**, 77 (1985).
27. J. Bauman and M. D. Fayer, *J. Chem. Phys.* **85**, 4087 (1986).
28. B. B. Mandelbrot, *The Fractal Geometry of Nature* (Freeman, San Francisco, 1983).
29. R. Kopelman, *Science* **241**, 1620 (1988).
30. P. Levitz, J. M. Drake, J. Klafter, *J. Chem. Phys.* **89**, 5224 (1988).
31. P. Levitz and J. M. Drake, *Phys. Rev. Lett.* **58**, 686 (1987).
32. C. L. Yang, P. Evesque, M. A. El-Sayed, in (*11*), pp. 371–386.
33. P. Levitz, J. M. Drake, J. Klafter, *Chem. Phys. Lett.* **148**, 557 (1988).
34. A. Blumen, J. Klafter, G. Zumofen, *J. Chem. Phys.* **84**, 1387 (1986).
35. P. Levitz and J. M. Drake, in preparation.
36. Ö. Peckan, M. A. Winnik, M. D. Croucher, *Phys. Rev. Lett.* **61**, 641 (1988).
37. ———, *Chem. Phys.* **146**, 283 (1990).
38. J. M. Drake, P. Levitz, S. Sinha, *Mater. Res. Soc. Symp. Proc.* **73**, 305 (1986).

39. We are grateful to A. Blumen, G. Zumofen, and S. Sinha for fruitful collaboration and discussions.